Korean J. Chem. Eng., **27**(4), 1184-1191 (2010)
DOI: 10.1007/s11814-010-0177-8

Investigation of equilibrium and kinetic parameters of methylene blue adsorption onto MCM-41

Purushothaman Monash and Gopal Pugazhenthi†

Department of Chemical Engineering, Indian Institute of Technology Guwahati, Guwahati 781039, India
(*Received 25 June 2009 • accepted 8 November 2009*)

Abstract−Mesoporous MCM-41 was synthesized at room temperature using tetraethoxysilane (TEOS) with cetyltrimethylammonium bromide (CTAB) and employed as an effective adsorbent for the adsorption of methylene blue dye from aqueous solution. The as-synthesized MCM-41 was calcined at 250 and 550 °C to study the relation between the surface area and pore volume with surfactant removal. The synthesized MCM-41 was characterized using thermo gravimetric analysis (TGA), X-ray diffraction (XRD) patterns, nitrogen adsorption/desorption isotherms and Fourier transform infrared (FT-IR) spectroscopy. The MCM-41 calcined at 550 °C showed higher surface area (1,059 $m^2 g^{-1}$) with pore volume of 0.89 ml g^{-1} and was used for the investigation of adsorption isotherms and kinetics. The experimental results indicated that the Freundlich and Redlich-Peterson models expressed the adsorption isotherm better than the Langmuir model. In addition, the influence of temperature and pH on adsorption was also investigated. The decrease in temperature or the increase in pH enhanced the adsorption of dye onto MCM-41. A maximum adsorption capacity of 1.5×10^{-4} mol g^{-1} was obtained at 30 °C. The kinetic studies showed that the adsorption of dye on MCM-41 follows the pseudo-second-order kinetics.

Key words: Adsorption, Methylene Blue, MCM-41, Isotherm, Kinetic

INTRODUCTION

The dyestuff effluents produced from industries such as textile, paper, printing, leather, food, and cosmetics exhibit toxic and carcinogenic effects on mammals and aquatic lives [1,2]. The color present in the effluent is a continuing problem for dyestuff manufacturers that creates numerous environmental issues. Methylene blue is one of the most widely used dyes in the textile industry. It creates harmful effects such as rapid or difficult breathing on inhalation. It may cause nausea, vomiting, diarrhea, gastritis and also creates abdominal pain, chest pain, severe headache, etc., on ingestion through the mouth [3]. Various methods have been reported for the treatment of the dyes with each of them having advantages and disadvantages [2,4]. Among the various methods, adsorption is found to be a versatile process and gives the best results for the removal of dyes, especially using activated carbon as an adsorbent. However, the cost of activated carbon is high and difficult to regenerate, which makes necessary a search for a new class of adsorbents. Several researchers have worked on non-conventional low-cost adsorbents, including natural materials, biosorbents, industrial and agricultural waste materials for the dye removal from aqueous solution [2,5]. Methylene blue (MB) adsorption on various sorbents was also reported in many literatures [1,3, 6-9].

Researchers from the Mobil Oil Corporation synthesized a series of novel, mesoporous aluminosilicates, in which MCM-41 was a novel mesoporous zeolite having cylindrical pore structure and high degree of pore symmetry. The large surface area and its nanometer-sized pore make it an ideal material for catalyst applications and also testing for various adsorption and diffusion models [10,14]. The main advantage of MCM-41 is that it can be regenerated by simple washing with alkaline or acid solution to recover the adsorbents and adsorbed dyes [14]. Generally, MCM-41 is prepared under alkaline conditions at high temperature using an autoclave reactor. Zhao et al., have synthesized MCM-41 using different silica precursors [10]. The effect of various silica precursors, cationic templates and surfactant chain length was reported and MCM-41 showed different surface properties depending on the synthesis methodology [11-13]. Most of the reported adsorption studies on MCM-41 have concentrated on gases and only very few works have been reported for liquid systems [14]. A few investigations were found for the adsorption of MB on MCM-41 synthesized using high pressure autoclave hydrothermal reaction [14,15-17]. However, to the best of the authors' knowledge, adsorption of MB on room temperature synthesized MCM-41 and its adsorption capability has not yet been investigated.

The main objective of the present work is to investigate the potential of MCM-41 synthesized at room temperature for the removal of MB dye from aqueous solution. The influence of contact time, pH and temperature on adsorption characteristics of MCM-41 is studied and the experimental data obtained from the equilibrium studies are fitted to Langmuir, Freundlich and Redlich-Peterson adsorption models. In addition, kinetic studies are also carried out to determine the adsorption mechanism.

EXPERIMENTAL

Tetraethylorthosilicate (TEOS) and cetyltrimethylammonium bromide (CTAB, chemical formula=$C_{19}H_{42}BrN$, Mol.wt.=364.45) were purchased from Merck (Germany) and s.d Fine Chemicals (Mum-

†To whom correspondence should be addressed.
E-mail: pugal@iitg.ernet.in

bai, India). Ammonium hydroxide (25 wt%), ethanol, methylene blue (C.I. 52015, chemical formula=$C_{16}H_{18}N_3SCl$, Mol.wt.=319.86), sodium hydroxide (NaOH) and hydrochloric acid (HCl) were procured from Merck (I) Ltd (Mumbai, India). All the chemicals were used as received. Water used in the preparation of MCM-41 and dye solution was obtained from a Millipore System.

1. Adsorbent (MCM-41) Synthesis

MCM-41 was synthesized through modified classical synthesis method [18], by dissolving 2.4 g of CTAB in 120 ml of Millipore water and stirring the solution continuously by using a laboratory stirrer until a clear homogeneous solution was obtained. Then 10.2 ml of 25 wt% aqueous ammonia was added into the homogeneous solution and the mixture was stirred for 5 min. A required amount of TEOS was added drop by drop into the above mixture with stirring. The molar composition of the gel was 1 M TEOS : 3.089M NH_3 : 0.1358M CTAB : 137.54M H_2O. The mixture was stirred overnight to carry out the reaction. The white precipitate formed was filtered and washed consecutively with Millipore water and ethanol. The as-synthesized material was calcined at 250 and 550 °C for 5 h to remove the surfactant.

2. Characterization of MCM-41

Thermo gravimetric analysis (TGA) was performed on the Mettler Toledo thermo gravimetric analyzer (TGA/SDTA 851® model). The measurements were carried out under air atmosphere from 25 to 970 °C with a heating rate of 10 °C min^{-1}. The X-ray diffraction (XRD) patterns of MCM-41 samples were recorded under air atmosphere at room temperature on a Bruker AXS instrument equipped with Cu Kα (λ=1.5406 Å) radiation operating at 40 kV and 40 mA between 2θ in the range of 0.5 and 10 degree with a scan speed of 0.02° s^{-1}. Nitrogen adsorption/desorption isotherms of MCM-41 samples were measured at −196 °C by Beckmen-Coulter surface area analyzer (SA™ 3100 model). All the MCM-41 samples were degassed at 150 °C for 4 h, prior to the N_2 adsorption/desorption analysis. The surface area was calculated by using a multipoint Brunauer-Emmett-Teller (BET) model. The pore size distribution was obtained through the BJH model using the desorption isotherms, and the total pore volume was estimated at a relative pressure of 0.99, assuming full surface saturation with nitrogen. The morphology of the synthesized MCM-41 materials was inspected by scanning electron microscopy (SEM) (LEO 1430VP® model). FT-IR spectra were recorded between 4,000 and 450 cm^{-1} region using spectroscopic quality KBr powder with a Perkin-Elmer spectrometer (spectrum one model). To estimate the pH of MCM-41 samples, a digital pH meter (Century CP 901) was used and the following procedure was adopted. A 0.5 g of the mesoporous sample was mixed with 10 ml of Millipore water and shaken for 24 h at 30 °C. After 24 h, the solution was filtered and the pH of the filtrate was determined with the digital pH meter.

3. Equilibrium Studies

Adsorption isotherm studies were carried out using the above synthesized MCM-41 (calcined at 550 °C) as an adsorbent by batch equilibrium technique. The dye was first dried at 100 °C for 2 h to remove any moisture. A stock solution of concentration 1.25×10^{-3} M was prepared and the experimental solutions of the desired concentration were obtained by successive dilutions of the stock solution. For adsorption isotherm experiments, 50 ml of dye solution of known initial concentrations in the range of 3.12×10^{-5} to 6.25×10^{-4} M was shaken with 0.02 g of MCM-41 in an incubator shaker (Labtech®, Korea) at 100 rpm. The pH of the dye solution was kept at 5.86 without changing (pH of the freshly prepared dye solution). The solution and solid phase were separated by centrifugation at 8,000 rpm for 30 min in a high speed refrigerated table top centrifuge (Sigma Laborzentrifugen Gmbh, Model 4k15C). About 10 ml of the supernatant was collected without disturbing the centrifuged solution and analyzed spectrophotometrically by measuring the maximum absorbance at the wavelength, λ_{max}, of 664 nm. The experiments were carried out at three different temperatures (30, 40, and 50 °C). The amount of MB adsorbed on MCM-41 at equilibrium was obtained by the following expression.

$$q_e = \frac{V\times(C_0 - C_e)}{m} \quad (1)$$

where q_e is the amount of dye adsorbed at equilibrium (mol g^{-1}), V is the volume of the solution (dm^3), m is the mass of the adsorbent (g), C_0 and C_e are the initial and equilibrium concentrations of the dye, respectively, computed from the calibration curve.

4. Kinetic Studies

The effect of contact time on the amount of dye adsorbed was investigated at one fixed initial dye concentration (3.13×10^{-4}) by adding 50 ml of dye solution to 0.02 g of MCM-41. The mixture was shaken as a function of time in an incubator shaker at 100 rpm at three different temperatures. At various time intervals, samples were taken and the concentration was measured. The amount of MB adsorbed q_t at time t was determined by the following expression.

$$q_t = \frac{V\times(C_0 - C_t)}{m} \quad (2)$$

where q_t is the amount of dye adsorbed at time t (mol g^{-1}), V is the volume of the solution (dm^3), m is themass of the adsorbent (g), C_0 and C_t are the concentrations of the dye at initial (t=0) and at time t, respectively.

5. Effect of pH

The influence of pH on dye removal was determined by performing the adsorption experiments at different initial pH of the solution (2-11) for three different temperatures (30, 40 and 50 °C). The pH of the solution was adjusted by adding a few drops of NaOH or HCl to reach the desirable value, before shaking. All the adsorption experiments were always done in duplicate and the mean values were taken. The percentage difference was calculated and plotted as error (as positive and negative error) for the experimental data.

RESULTS AND DISCUSSION

1. Characterization of MCM-41 Adsorbent

Thermo gravimetric analyses of the as-synthesized and calcined MCM-41 samples are shown in Fig. 1. The as-synthesized MCM-41 sampleshows the weight loss in three distinct regions. The removal of water molecules physisorbed on the external surface of the materials causes the first region of weight loss (28%) between 50 and 100 °C. The second region of weight loss (7%) between 100 and 280 °C is attributed to the decomposition of the surfactant. The third region of weight loss (24%) between 280 and 550 °C is due to the combustion of the surfactant and loss of water that is generated from the condensation of adjacent silanol groups. The MCM-

41 calcined at 250 °C shows the 8% weight loss between 50 and 120 °C, 20% weight loss between 120 and 380 °C due to breaking of the hydrocarbon chain of surfactant and the third region of weight loss is about 6% between 380 and 550 °C combustion of the surfactant and water loss associated with condensation of silanol groups. The MCM-41 calcined at 550 °C shows two regions of weight loss, and it is observed that only about 3% of weight loss is after 120 °C, which shows that the surfactant is completely removed from the MCM-41.

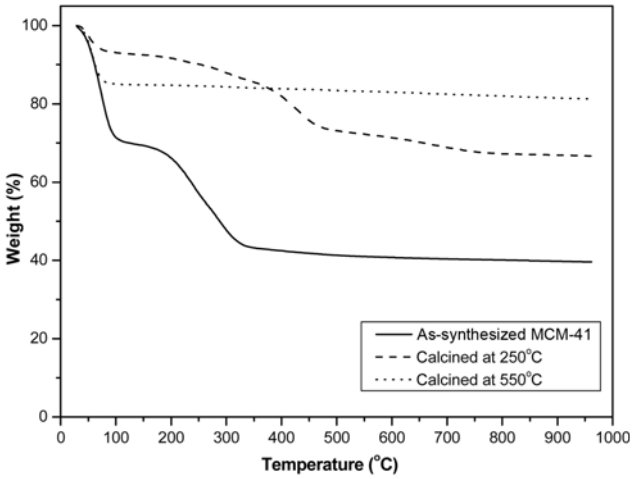

Fig. 1. Thermogravimetric analysis of MCM-41 samples.

Fig. 2 depicts the XRD patterns of the MCM-41 samples. Only one low-angle peak for d_{100} plane corresponding to the mesophase is observed in all the samples at 2θ value of 1.43°. This is mainly due to the length of the carbon chain used for synthesis (C_{19}), which is the characteristic of MCM-41 materials [13,19]. Since the materials are not crystalline at the atomic level, no reflections at higher angles are observed. The peak positions remained almost unchanged, which indicates that the structural order is not affected by calcination. The textural properties of the MCM-41 samples are reported in Table 1.

The nitrogen adsorption/desorption isotherms of the prepared MCM-41 are shown in Fig. 3. The isotherms observed for the different MCM-41 samples must be during calcinations the sample changes from a "type I-like" isotherm (as-synthesized) to a typical type IV isotherm (calcined at 550 °C), which is the characteristic of the mesoporous material according to the IUPAC nomenclature [20]. The MCM-41 calcined at 250 and 550 °C shows three distinct regions of N_2 adsorption isotherms. The MCM-41 calcined at 250 °C shows a linear increase of the adsorbed volume at low relative pressures (P/Po~0.2), which may be attributed to a monolayer-multilayer adsorption on the pore walls. For relative pressures between

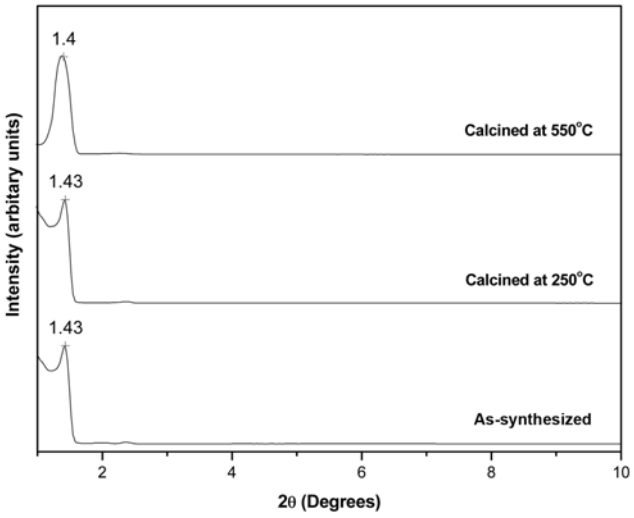

Fig. 2. XRD pattern of MCM-41 samples.

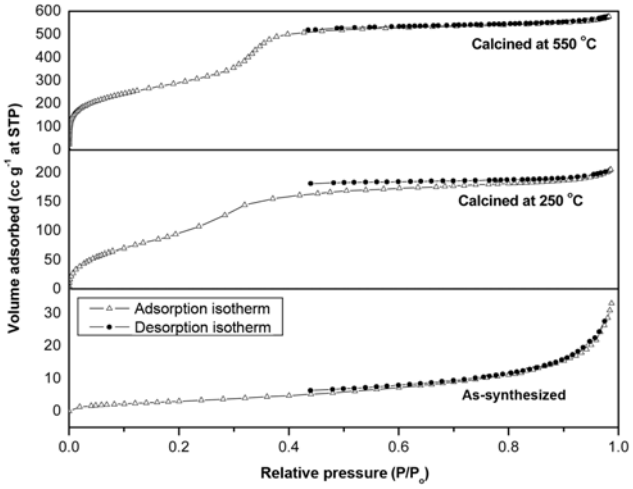

Fig. 3. Nitrogen adsorption/desorption isotherms of MCM-41 samples.

Table 1. Textural properties of MCM-41 samples

Sample	pHpzc	X-ray diffraction				N_2 adsorption		
		d_{100} Spacing (nm)	Unit cell parameter[a] a_o (nm)	Wall thickness[b] (nm)	Crystallite size (nm)	BET surface area ($m^2 g^{-1}$)	Specific pore volume (ml g^{-1})	Average pore diameter[c] Dp (nm)
As-synthesized	6.37	6.28	7.26	3.570	19.36	48.78	0.0450	3.690
Calcined at 250 °C	4.27	6.29	7.28	3.863	19.34	368.99	0.3134	3.397
Calcined at 550 °C	4.87	6.40	7.39	4.028	14.16	1059.33	0.8905	3.362

[a]Unit cell parameter $a_o = 2\, d_{100}/\sqrt{3}$. Where d_{100} is the d-spacing of (100) reflection

[b]Wall thickness $= a_o - D_p$

[c]Average pore diameter $D_p = 4V_{mes}/S_{BET}$. Where V_{mes} is the mesopore volume and S_{BET} is the BET surface area

0.2 and 0.42 a sharp increase in the adsorbed volume is observed which is due to capillary condensation of N_2 in the pore channels. A very small linear increase at higher relative pressures between 0.42 and 0.99 shows the multilayer adsorption on the outer surface. The MCM-41 calcined at 550 °C follows the same pattern as like as the MCM-41 calcined at 250 °C. However,the increase in N_2 uptake is even steeper at a relative pressure between 0.28 and 0.42, which indicates a much narrower pore size distribution. The surface area and pore volume are increased during calcination. The MCM-41 calcined at 550 °C obtains a relatively high surface area (1,059 $m^2 g^{-1}$) and pore volume (0.8905 ml g^{-1}).

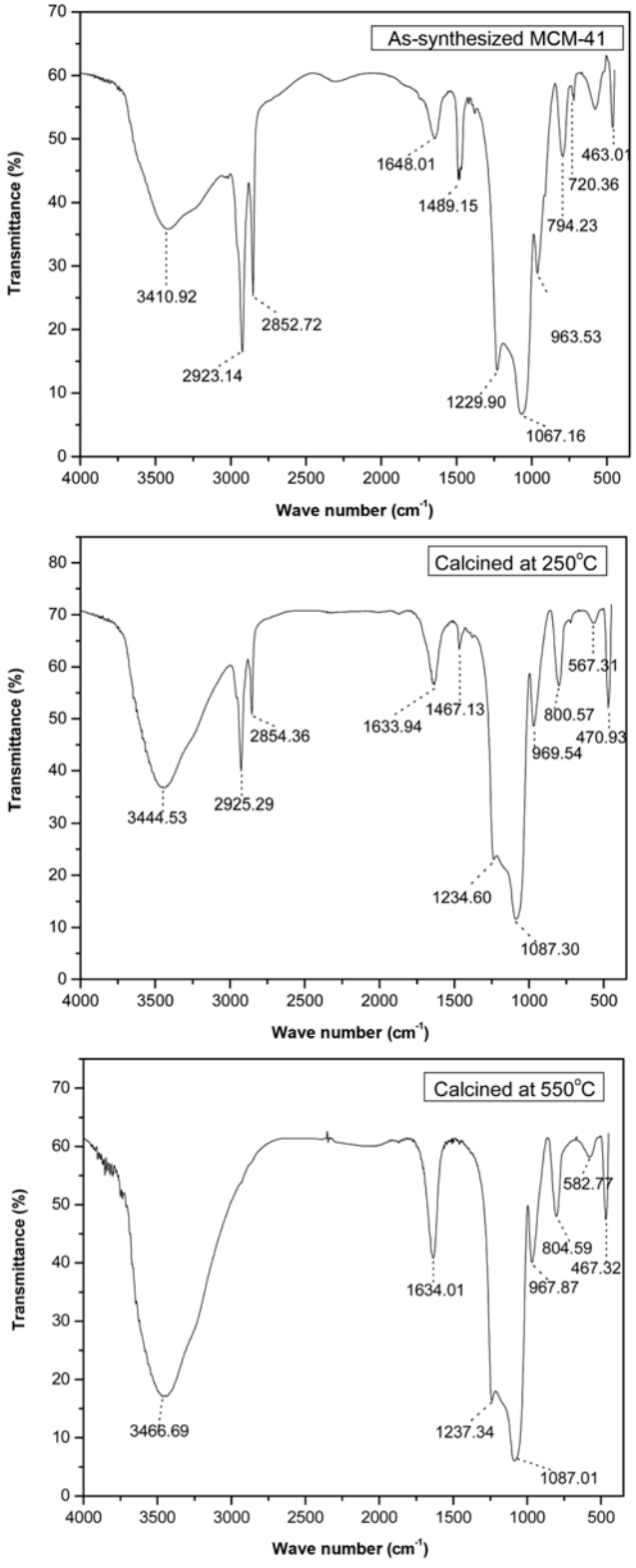

Fig. 4. FT-IR spectrum of MCM-41 samples.

Fig. 4 shows the FT-IR spectra of the as-synthesized and calcined samples of MCM-41. The as-synthesized sample shows two very sharp intense bands at 2,923 and 2,852 cm^{-1} that are due to the C-H stretching of the hydrocarbon chain of the surfactant molecules. The corresponding bending vibration mode is observed at 1,489 cm^{-1}. In the hydroxyl region (3,600-3,200 cm^{-1}), a broad band is seen around 3,410 cm^{-1}, which is attributed to surface silanols and adsorbed water molecules. The absorption bands close to 1,648 cm^{-1} are due to the bending vibration of adsorbed water molecules. The asymmetric stretching vibrations of Si-O-Si are observed by the absorption bands at 1,067 and 1,230 cm^{-1}. The band at 970 cm^{-1} is attributed to Si-OH vibrations. The absorption peaks around 460 to 795 cm^{-1} are mainly due to bending vibration of Si-O-Si bonds and the band at 794 cm^{-1} may also correspond to free silica [20]. The spectrum of the sample calcined at 250 °C also shows the similar bands and the bond stretching properties. The C-H stretching bands at 2,923 and 2,852 cm^{-1} and its vibration mode observed at 1,489 cm^{-1} are as like that of as-synthesized sample, which confirms that the organic compound is not completely removed at 250 °C. All the bands belonging to the organic groups disappeared for the sample calcined at 550 °C, which proves the complete removal of the surfactants.

The pH of the as-synthesized, calcined at 250 and 550 °C MCM-41, is found to be 6.37, 4.27 and 4.87, respectively.

2. Adsorption Isotherms

The adsorption of the dye is performed using MCM-41 material calcined at 550 °C due to its higher surface area and pore volume (hereafter, MCM-41 refers to MCM-41 calcined at 550 °C sample). The equilibrium relationship between adsorbent and adsorbate can be described by adsorption isotherms. The adsorption isotherm expresses the relationship between the amount of dye adsorbed per unit mass of the adsorbent and the liquid phase dye concentration at constant temperature. Several adsorption isotherms are available in the present study, the adsorption isotherms of MB at different temperatures on MCM-41 are measured and fitted using three important isotherm models: Langmuir, Freundlich and Redlich-Peterson. The models are fitted in nonlinear form without linearization because linearization leads to an error (high or low correlation coefficient) value of correlation coefficients (R^2) depending on in which form it is linearized. So it is difficult to predict the actual isotherm. Nonlinear method is the best way to get the actual isotherm parameters [21].

The Langmuir isotherm is valid for monolayer adsorption onto a surface with a finite number of identical sites. The homogeneous Langmuir adsorption isotherm is represented by the following equation [22].

$$q_e = \frac{Q_{max} K_L C_e}{(1 + K_L C_e)} \quad (3)$$

where q_e is the adsorbed amount of the dye at equilibrium (mol g^{-1}), C_e is the equilibrium concentration of the dye in solution (mol dm^{-3}),

is the maximum adsorption capacity (mol g^{-1}), and K_L is the constant related to the free energy of adsorption (dm^3 mol^{-1}).

The Freundlich isotherm is an empirical equation assuming that the adsorption process takes place on heterogeneous surfaces,and adsorption capacity is related to the concentration of MB at equilibrium. The heterogeneous Freundlich adsorption isotherm is represented by the following equation [23].

$$q_e = K_F C_e^{1/n} \quad (4)$$

where K_F is the Freundlich isotherm constant (mol/g $(dm^3/mol)^{1/n}$), which is indicative of the extent of adsorption (i.e., adsorption capacity) and 1/n is the adsorption intensity (dimensionless), which indicates the degree of nonlinearity between solution concentration.

The Redlich-Peterson isotherm has three parameters and it combines the features of both the Freundlich and Langmuir isotherm equations. Its adsorption mechanism does not obey ideal monolayer adsorption, but an impure one, i.e., it approaches the Freundlich model at high concentrations, and at low concentration it approaches to the Langmuir equation. The Redlich-Peterson isotherm can be described by the equation [24].

$$q_e = \frac{K_{RP} C_e}{1 + \alpha C_e^g} \quad (5)$$

where K_{RP} and α are the Redlich-Peterson constants and g is the exponent which lies between 0 and 1. For g=1, the above equation reduces to Langmuir form. This model can describe the adsorption process over a wide range of concentrations.

To determine the influence of temperature, adsorption studies of MB are performed at three different temperatures (30, 40 and 50 °C). The experimental data obtained are fitted with the three isotherm models and the parameters obtained from these models are listed in Table 2. The adsorption isotherms at different temperature are fitted very well with all the three models, and the regression coefficients (R^2) obtained for the Freundlich and Redlich-Peterson model (>0.991) are greater than the Langmuir model (0.905-0.952). The best fitted Redlich-Peterson model is shown in Fig. 5 (other models not shown here). The maxmium adsorption capacity obtained from the langmuir modelis found to be higher at 30 °C (1.5×10^{-4} mol g^{-1}) as compared tohigher temperatures (1.3×10^{-4} mol g^{-1} at 40 °C and 1.1×10^{-4} mol g^{-1} at 50 °C). The higher K_L value at 30 °C indicates higher solute adsorptivity due to higher binding energy between MB dye and MCM-41. This indicates that the adsorption is more at lower temperature than higher temperature for the adsorption of MB dye on MCM-41. However, that the variation in the maximum adsorption capacity is less for the studied temperature indicates that the temperature has less effect on adsorption. The higher value of K_F indicates that higher extension of uptake of MB at 30 °C and the lower value of 1/n at all temperatures signifies that the forces which are exerted on the surface of the MCM-41 during MB dye adsorption are weak. The greater values of n (>5) indicates the degree of favorability of adsorption of MB dye on MCM-41.The value of g obtained from Redlich-Peterson model ranging between 0 and 1 indicates a favorable adsorption. Table 3 shows the comparison of the maximum adsorption capacity, Q_{max}, of the present study with the other adsorbents reported in the literature. The maximum adsorption capacity of 1.5×10^{-4} mol g^{-1} obtained in this work is greater than the value (3.75×10^{-5} mol g^{-1}) reported by Wang and Li [17].

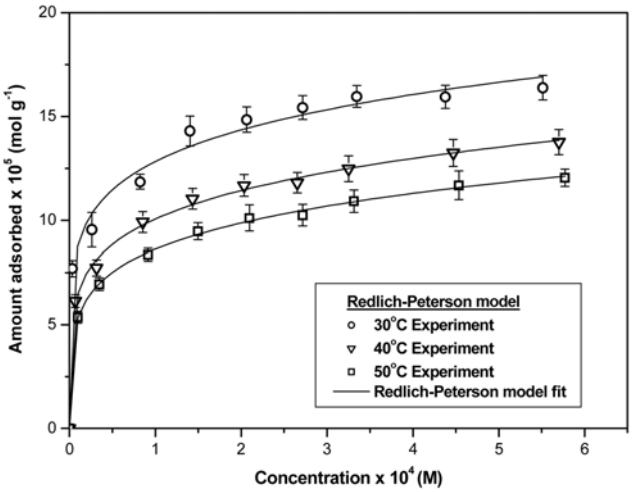

Fig. 5. Best fitted Redlich-Peterson model for the adsorption of MB dye on MCM-41 at different temperatures.

3. Effect of pH

The pH of the solution is an important controlling parameter in the adsorption process. The point of zero charge (PZC) is also an important parameter in determining the adsorption characteristics

Table 2. Parameters of adsorption isotherms of MB on MCM-41 at different temperatures

Isotherm model	Parameters	Temperature (°C)		
		30	40	50
Langmuir model	Q_{max} (mol g^{-1})	1.5×10^{-4}	1.3×10^{-4}	1.1×10^{-4}
	K_L (dm^3 mol^{-1})	17.35×10^{4}	7.66×10^{4}	5.63×10^{4}
	R^2	0.905	0.940	0.952
Freundlich model	K_F (mol/g$(dm^3/mol)^{1/n}$)	5.7×10^{-4}	5.5×10^{-4}	5.4×10^{-4}
	1/n	0.161	0.185	0.198
	R^2	0.991	0.998	0.999
Redlich-peterson model	K_{RP} (mol g^{-1})	6.53×10^{2}	5.27×10^{2}	1.45×10^{2}
	α ((dm^3 mol^{-1})^g)	8.68×10^{5}	9.73×10^{5}	2.84×10^{5}
	g	0.851	0.817	0.807
	R^2	0.998	0.998	0.999

Table 3. Adsorption capacity of various adsorbent for MB

Adsorbent	Adsorption capacity (mol g^{-1})	Reference
Raw kaolin	4.37×10^{-5}	(3)
Pure kaolin	4.85×10^{-5}	(3)
Activated carbon from coconut husk	2.68×10^{-4}	(25)
Activated carbon - commericial F400	1.30×10^{-4}	(26)
Activated carbon from coconut shell	5.24×10^{-5}	(27)
Diatomite	1.47×10^{-4}	(28)
Natural zeolite	4.50×10^{-5}	(29)
MCM-22	1.80×10^{-4}	(29)
MCM-48	3.27×10^{-5}	(17)
MCM-50	6.87×10^{-5}	(17)
MCM-41	3.75×10^{-5}	(17)
MCM -41	1.50×10^{-4}	Present work

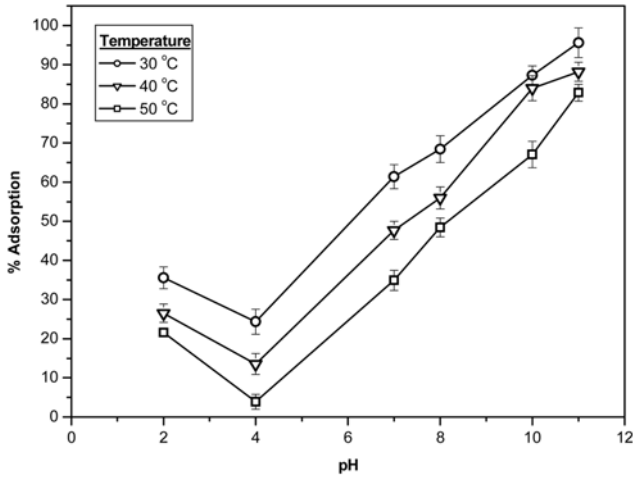

Fig. 6. Effect of pH of MB adsorption at different temperatures with an initial MB.

of MB dyes on MCM-41. Although acid/base titration method is widely used to determine the PZC, the PZC of MCM-41 adsorbent is found by an effective method that states the pH of MCM-41 slurry is considered as point of zero charge (pHpzc) [17,30,31]. The pHpzc of the MCM-41 samples are presented in Table 1. Generally, favorable adsorption of an MB dye on MCM-41 will take place when the solution pH is greater than pHpzc. Fig. 6 depicts the influence of pH on MB adsorption onto MCM-41 at different temperatures. At higher pH (4-11), the pH of the solution is higher than pHpzc of the adsorbent (4.87), which generally favors the adsorption of MB (cationic) on MCM-41. The increased adsorption at higher pH (greater than pHpzc) is mainly due to enhanced association of the dye cations. It is related to the electrostatic attraction force of the dye compound with MCM-41. Increase in the pH of the solution increases the electrostatic attraction between the positively charged dye and the surface of the adsorbent, which results in increased adsorption of MB dye. Similar observations were previously reported for the adsorption of MB on other adsorbents [3,27,32]. At lower pH (pH=2), the dissociation of the MB dye molecules takes place that leads to an increased adsorption at pH=2 [14,15]. Lee et al. [15] have also reported a similar type of observation for the influence of pH on adsorption of methylene green (cationic dye) onto MCM-41.

4. Kinetic Studies

Adsorption kinetics of MB is studied to provide information about the mechanism of adsorption, which is important for the efficiency of the process. Several adsorption kinetic models are available in this work, the pseudo-first-order Lagergren equation and pseudo-second-order rate equation are fitted with the experimental data. The pseudo-first order rate expression is generally described by the following equation [33].

$$\frac{dq_t}{dt} = k_1(q_e - q_t) \tag{6}$$

where k_1 is the pseudo-first-order rate constant (min^{-1}), q_e and q_t are the amount of dye adsorbed at equilibrium (mol g^{-1}) and at time t (mol g^{-1}), respectively. Eq. (6) can be transformed into nonlinear forms to predict the adsorption equilibrium.

$$q_t = q_e\,(1-\exp(-k_1 t)) \tag{7}$$

The pseudo-second-order rate equation can be explained by the following equation [34].

$$\frac{dq_t}{dt} = k_2(q_e - q_t)^2 \tag{8}$$

where k_2 is the rate constant of pseudo-second-order adsorption mechanism (g mol^{-1} min^{-1}). Integrating and applying boundary conditions t=0 and q_t=0 to t=t and q_t=q_e, and rearranging Eq. (8) becomes,

$$\frac{t}{q_t} = \frac{1}{k_2 q_e^2} + \frac{1}{q_e}t \tag{9}$$

Fig. 7 depicts the best fitted second-order kinetic model for the adsorption of MB dye on MCM-41 at different temperature (other models not shown here). The kinetic parameters obtained for the adsorption of MB on MCM-41 using the pseudo-first-order, pseudo-second-order, and diffusion model are presented in Table 4. It is observed from Table 4 that the experimental data of the equilib-

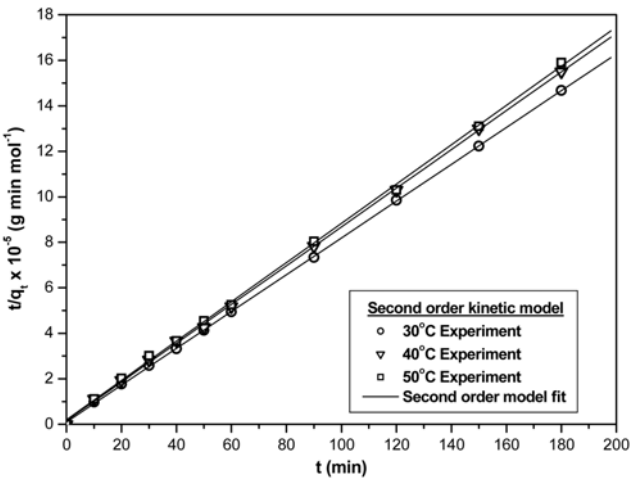

Fig. 7. Best fitted second-order kinetic model for the adsorption of MB dye on MCM-41 at different temperature.

Table 4. Parameters of kinetic models of MB adsorption on MCM-41 at different temperatures

T (°C)	$q_{e,exp}$ (mol g^{-1})	Pseudo-first-order kinetic model			Pseudo-second-order kinetic model			Diffusion model	
		k_1 (min^{-1})	q_e (mol g^{-1})	R^2	k_2 (g mol^{-1} min^{-1})	q_e (mol g^{-1})	R^2	K_d	R^2
30	1.50×10^{-4}	0.176	1.12×10^{-4}	0.980	6.3×10^{3}	1.4×10^{-4}	0.999	1.54×10^{-6}	0.791
40	1.24×10^{-4}	0.144	1.01×10^{-4}	0.989	4.6×10^{3}	1.15×10^{-4}	0.999	1.94×10^{-6}	0.771
50	1.12×10^{-4}	0.146	0.91×10^{-4}	0.981	3.7×10^{3}	1.01×10^{-4}	0.999	2.10×10^{-6}	0.830

rium adsorption matches very well with pseudo-second-order than pseudo-first-order kinetic model. Also, the regression coefficients for the pseudo-second-order model are greater than 0.99, which suggests that the adsorption mechanism is well explained by the pseudo-second-order kinetic model. Several researchers have already reported the selection of kinetic model based on the regression coefficient for adsorption of dyes [14,15,17].

In general, adsorption of dyes from the bulk solution to the porous adsorbent involves intra-particle diffusion and it may also be the rate limiting step in many adsorption processes. The intra-particle diffusion model is commonly used to identify the steps involved during adsorption. The diffusion model involves two steps, which suggests that the adsorption process proceeds by surface sorption and intraparticle diffusion. The diffusion model is expressed by the following equation [8].

$$q_t = k_d t^{1/2} + c \quad (10)$$

where k_d is the diffusion coefficient and c is the intercept indicating the boundary-layer surface sorption. In general, the first curved portion that appears in adsorption is due to the boundary-layer effect, and the second linear portion of the isotherm plot appears due to intraparticle or pore diffusion [29]. The obtained plot (not shown here) suggests that the adsorption process proceeds by surface adsorption and intraparticle diffusion. It can be seen from the Table 4 that the diffusion coefficient increases with anincrease of temperature (1.54×10^{-6} to 2.10×10^{-6} from temperature 30 to 50 °C), indicating the mobility of MB dye molecule onto MCM-41. However, there is a decrease in the amount of MB adsorbed onto MCM-41 with an increase of temperature which may be due to the collapse in the structure of the MCM-41 after dye adsorption.

CONCLUSIONS

Classical synthesis procedure has been successfully adopted for the preparation of MCM-41 at room temperature. The as-synthesized, calcined at 250 and 550 °C MCM-41 are characterized using XRD, TGA, SEM, FT-IR and N_2 adsorption/desorption isotherms. It is observed that the surfactant is completely removed at 550 °C. Maximum surface area of 1,059 m^2 g^{-1} is obtained for MCM-41 calcined at 550 °C as compared to the as-synthesized (49 m^2 g^{-1}) and calcined at 250 °C (369 m^2 g^{-1}) MCM-41. Investigation of the XRD pattern shows that there is no shift in peak position, which confirms that the structural stability is not affected during calcination. Higher adsorption capacity (1.5×10^{-4} mol g^{-1}) is obtained at 30 °C and it decreases with increase in temperature. The adsorption capacity increases with an increase of pH. The adsorption isotherm is well fitted with Freundlich and Redlich-Peterson model compared to that of the Langmuir model. The kinetic study confirmed that the adsorption of MB dye on MCM-41 follows pseudo-second-order model.

ACKNOWLEDGEMENT

The authors are thankful to the Centre for Nanotechnology and Department of Chemistry, IIT Guwahati for helping in XRD and FTIR analysis, respectively.

REFERENCES

1. V. K. Garg, M. Amita, R. Kumar and R. Gupta, *Dyes and Pigments*, **63**, 243 (2004).
2. G. Crini, *Bioresour. Technol.*, **97**, 1061 (2006).
3. D. Ghosh and K. G. Bhattacharyya, *Appl. Clay Sci.*, **20**, 295 (2002).
4. C. H. Liu, J. S Wu, H. C. Chiu, S. Y. Suen and K. H. Chu, *Water Res.*, **41**, 1491 (2007).
5. C. Namasivayam and S. Sumithra, *J. Environ. Manage.*, **74**, 207 (2005).
6. G. Kahr and F. T. Madsen, *Appl. Clay Sci.*, **9**, 327 (1995).
7. M. Dogan, M. Alkan, A. Turkyilmaz and Y. Ozdemir, *Water, Air, Soil Pollut.*, **184**, 229 (2000).
8. N. Kannan and M. M. Sundaram, *Dyes and Pigments*, **51**, 25 (2001).
9. A. Gurses, S. Karaca, C. Dogar, R. Bayrak, M. Acikyildiz and M. Yalcin, *J. Colloid Interface Sci.*, **269**, 310 (2004).
10. X. S. Zhao, G. Q. Lu and G. J. Millar, *Ind. Eng. Chem. Res.*, **35**, 2075 (1996).
11. P. B. Amama, S. Lim, D. Ciuparu, L. Pfefferle and G. L. Haller, *Microporous Mesoporous Mater.*, **81**, 191 (2005).
12. L. Huang, Q. Huang, H. Xiao and M. Eic, *Microporous Mesoporous Mater.*, **98**, 330 (2007).
13. H. P. Lin, S. Cheng and C. Y. Mou, *Microporous Mater.*, **10**, 111 (1997).
14. L. C. Juang, C. C. Wang and C. K. Lee, *Chemosphere*, **64**, 1920 (2006).
15. C. K. Lee, S. S. Liu, L. C. Juang, C. C. Wang, K. S. Lin and M. D. Lyu, *J. Hazard. Mater.*, **147**, 997 (2007).
16. Y. Ho, G. McKay and K. L. Yeung, *Langmuir*, **19**, 3019 (2003).
17. S. Wang and H. Li, *Microporous Mesoporous Mater.*, **97**, 21 (2006).
18. D. Kumar, K. Schumacher, C. F. Hohenesche, M. Grun and K. K. Unger, *Colloids Surf., A.*, **187**, 109 (2001).
19. O. Kaftan, M. Acikel, A. E. Eroglu, T. Shahwan, L. Artok and C. Ni, *Anal. Chim. Acta*, **547**, 31 (2005).
20. M. Ghiaci, A. Abbaspur, R. Kia, C. Belve, R. Trujillano, V. Rives and M. A. Vicente, *Catal. Commun.*, **8**, 49 (2007).
21. K. Vasanth Kumar, *Dyes and Pigments*, **74**, 595 (2006).
22. I. Langmuir, *J. Am. Chem. Soc.*, **27**, 1139 (1915).
23. H. Freundlich, *J. Phys. Chem.*, **57**, 385 (1907).

24. O. J. Redlich and D. L. Peterson, *J. Phys. Chem.*, **63**, 1024 (1959).
25. N. Graham, X. G. Chen and S. Jayaseelan, *Water Sci. Technol*., **43**, 245 (2001).
26. D. C. W. Tsang, J. Hu, M. Y. Liu, W. Zhang, K. C. K. Lai and I. M. C. Lo, *Water, Air, Soil Pollut*., **184**, 141 (2007).
27. K. P. Singh, D. Mohan, S. Sinha, G. S. Tondon and D. Gosh, *Ind. Eng. Chem. Res*., **42**, 1965 (2003).
28. J. X. Lin, S. L. Zhan, M. H. Fang and X. Q. Qian, *J. Porous Mater*., **14**, 449 (2007).
29. S. Wang, H. Li and L. Xu, *J. Colloid Interface Sci*., **295**, 71 (2006).
30. S. B. Wang and G. Q. Lu, *Carbon*, **36**, 283 (1998).
31. J. S. Noh and J. A. Schwarz, *J. Colloid Interface Sci*., **130**, 157 (1989).
32. V. K. Gupta, Suhas, I. Ali and V. K. Saini, *Ind. Eng. Chem. Res*., **43**, 1740 (2004).
33. S. Lagergren, *Kungl. Sven. Veten. Akad. Handl.*, **24**, 1 (1898).
34. Y. S. Ho and G. McKay, *Process Biochem*., **34**, 451 (1999).